

Thermal Behavior of Long-chain Alkanoylcholine Soaps

Ainhoa Tolentino,¹ Abdelilah Alla,¹ Antxon Martínez de Ilarduya,¹
Mercè Font-Bardia,² Salvador León,³ and Sebastián Muñoz-Guerra^{1*}

¹Departament d'Enginyeria Química, Universitat Politècnica de Catalunya, ETSEIB,
Diagonal 647, Barcelona 08028, Spain.

²Centre Científic i Tecnològic (CCiTUB), Universitat de Barcelona
Sole Sabaris 1-3, Barcelona 08028, Spain

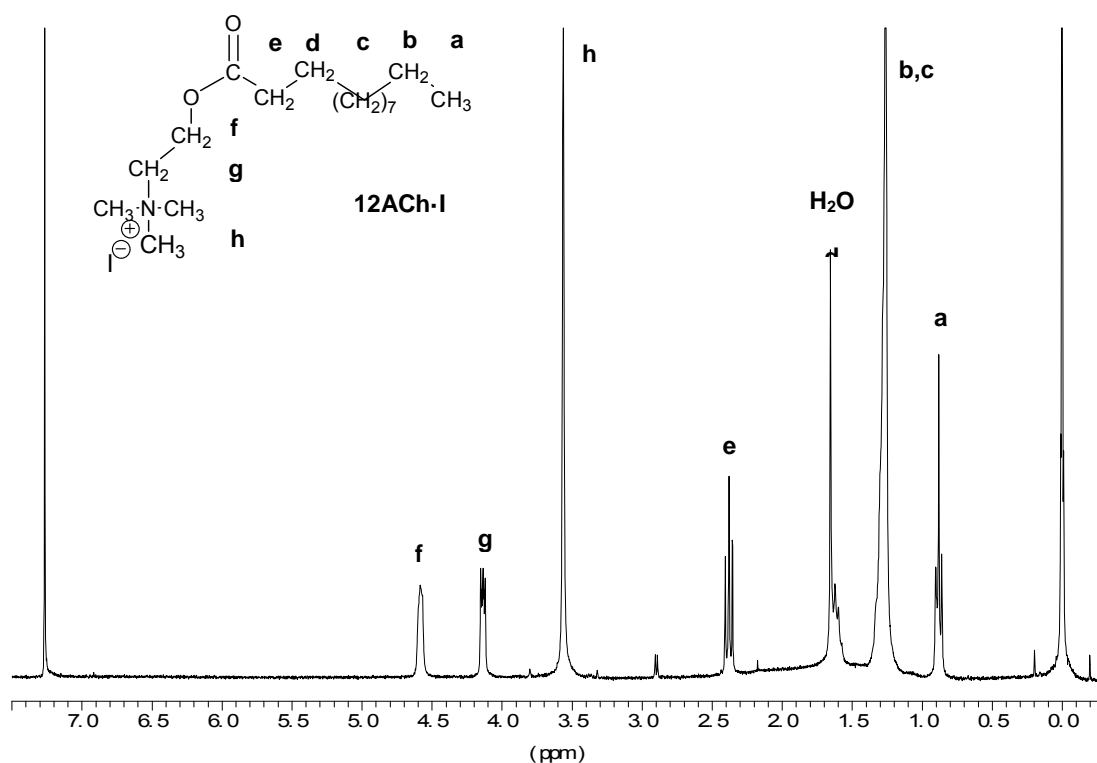
³Departamento de Ingeniería Química, Universidad Politécnica de Madrid, ETSIIM,
Gutierrez Abascal 2, Madrid 28006.
E-mail: sebastian.munoz@upc.edu.

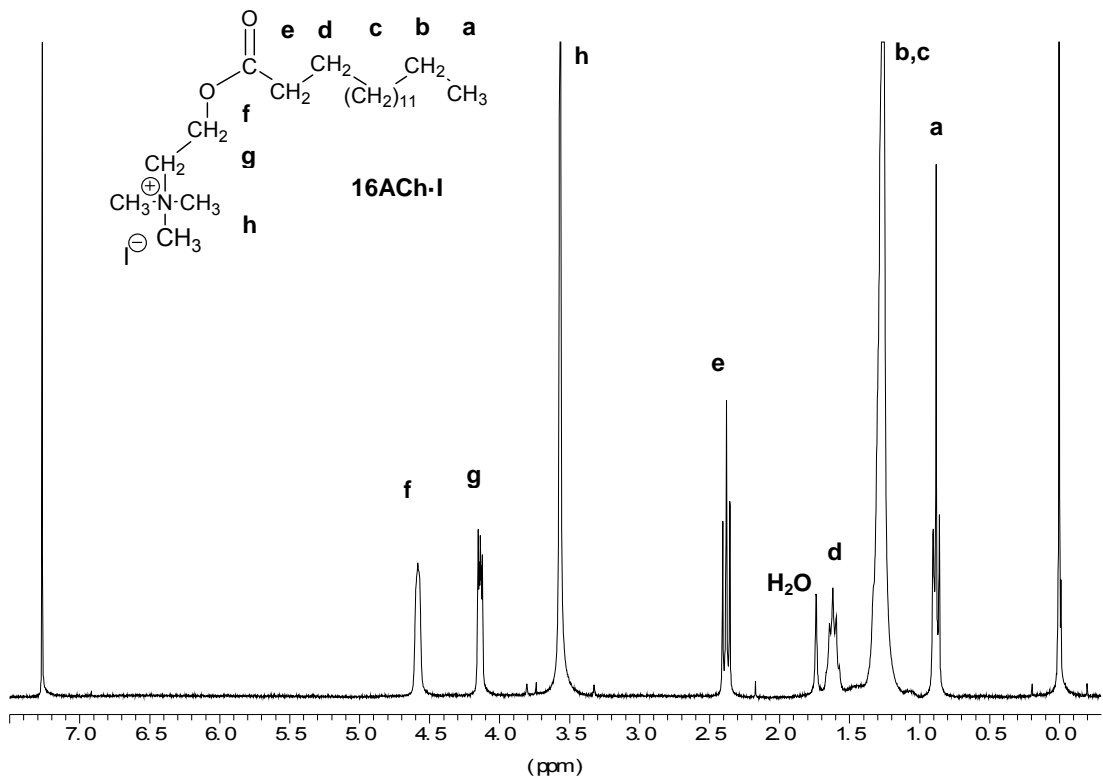
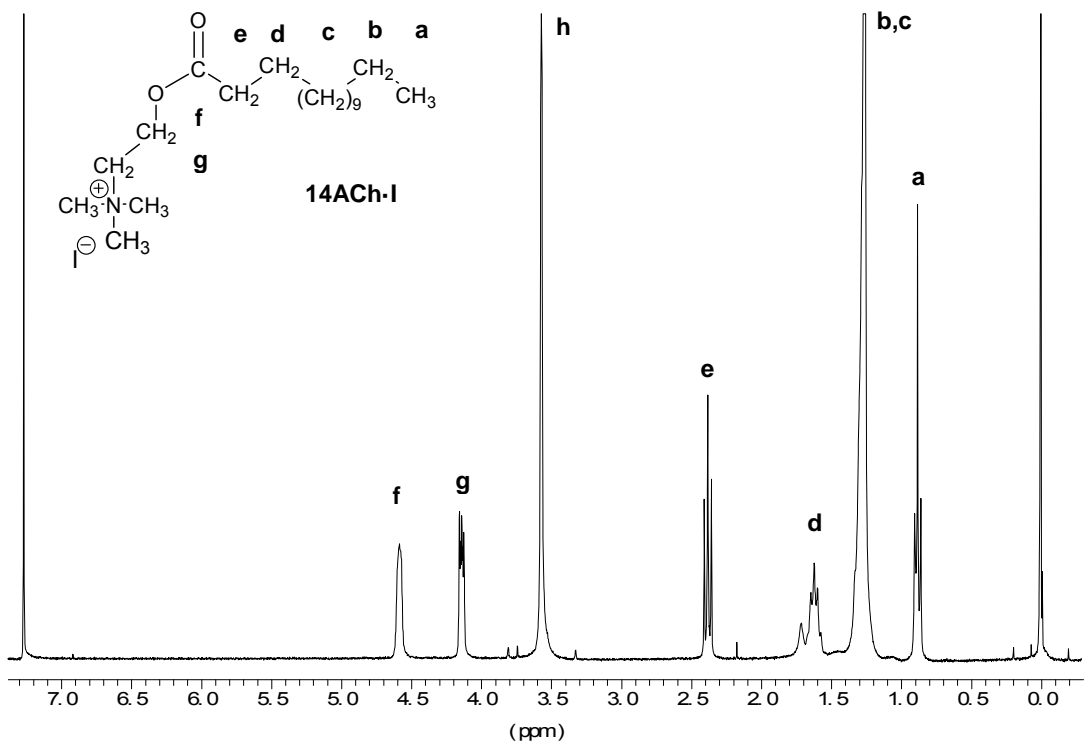
Supporting information file includes complementary data of *n*ACh·I: synthesis data; ¹H-NMR spectra; TGA derivatives traces; DSC traces; detailed description of single-crystal analysis methodology; polarizing optical microscope and SEM images of crystals and monocrystals; real time X-ray data (SAXS and WAXS); ¹³C CP-MAS NMR spectral; POM pictures.

Table ESI-1. Synthesis data of alkanoylcholine iodides.

<i>n</i>	T ₁ ^a (°C)	T ₂ ^a (°C)	DMAE- <i>n</i> A	Yield (%)	Purity ^b (%)	<i>n</i> ACh·I
12	0	20	Clear oil (colorless)	25	99.5	White powder
14	0	20	Clear oil (colorless)	88	100	White powder
16	20	20	Clear oil (colorless)	97	100	White powder
18	20	40	Oily solid (brown)	94	100	White powder

T₁ and T₂: reaction temperatures used at the 1st step (esterification) and 2nd step (quaternization). ^bEstimated by ¹H NMR.





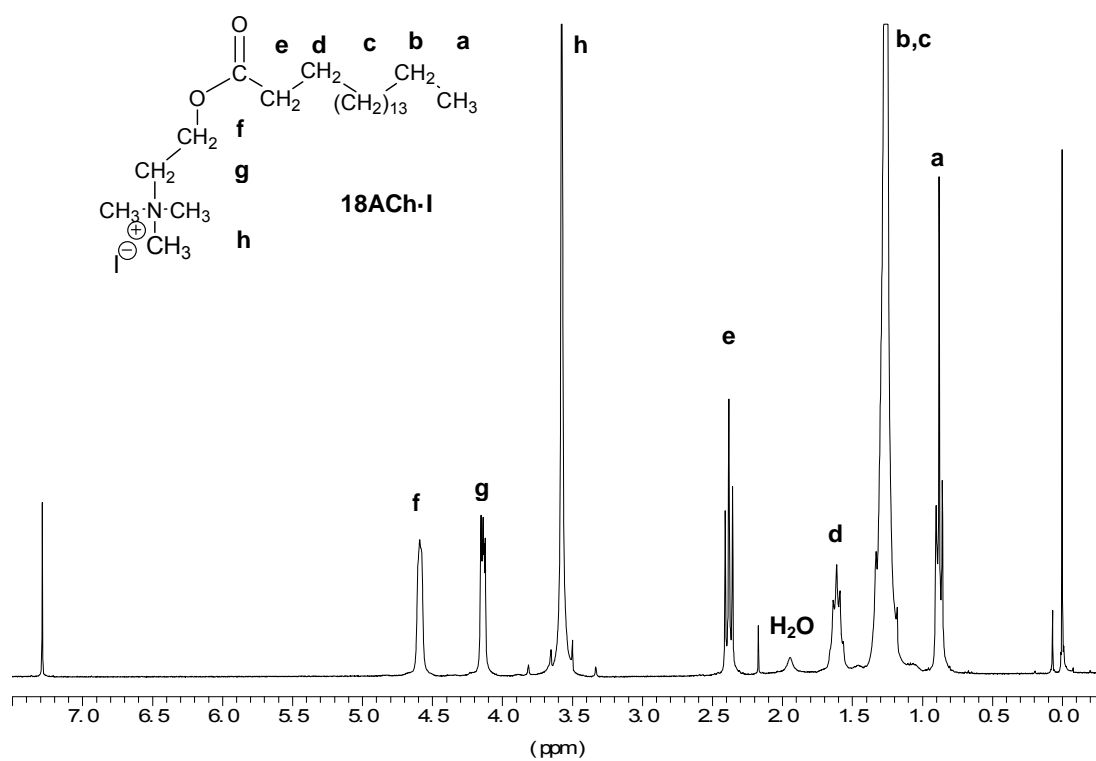


Figure. ESI-1. ¹H-NMR of *n*ACh-I series.

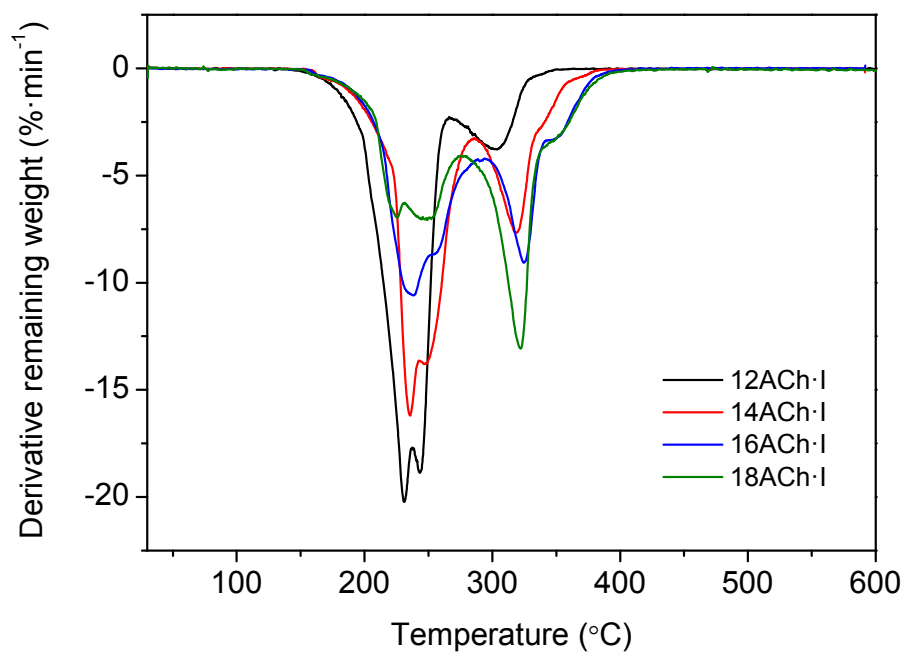


Figure ESI-2. TGA derivatives of *n*ACh-I series.

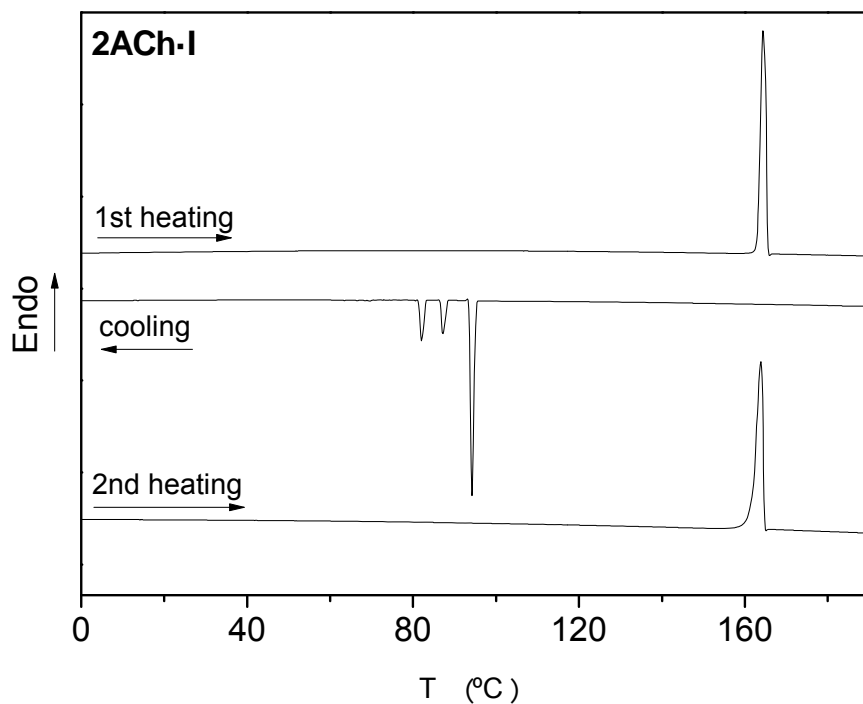


Figure ESI-3. DSC traces of acetylcholine iodide.

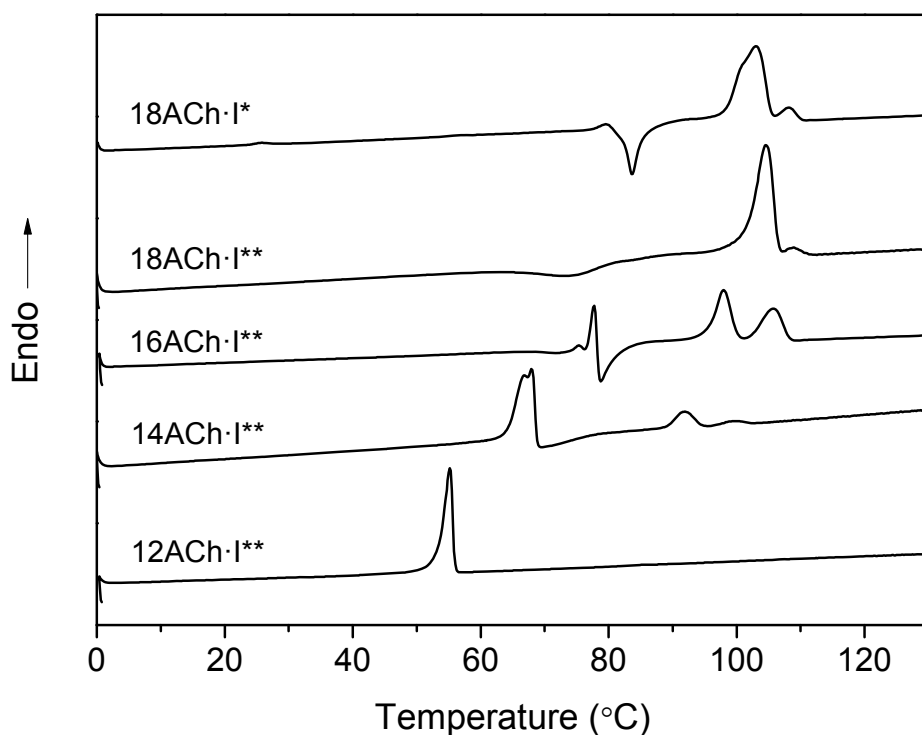


Figure ESI-4. DSC reheating traces of n ACh·I previously heated at temperatures below T_2 . (**) The Ph- β is present in 12, 14 and 16ACh·I whereas 18ACh·I is in Ph- α form. (*) Trace of 18ACh·I from a sample heated below T_2 for 2 h.

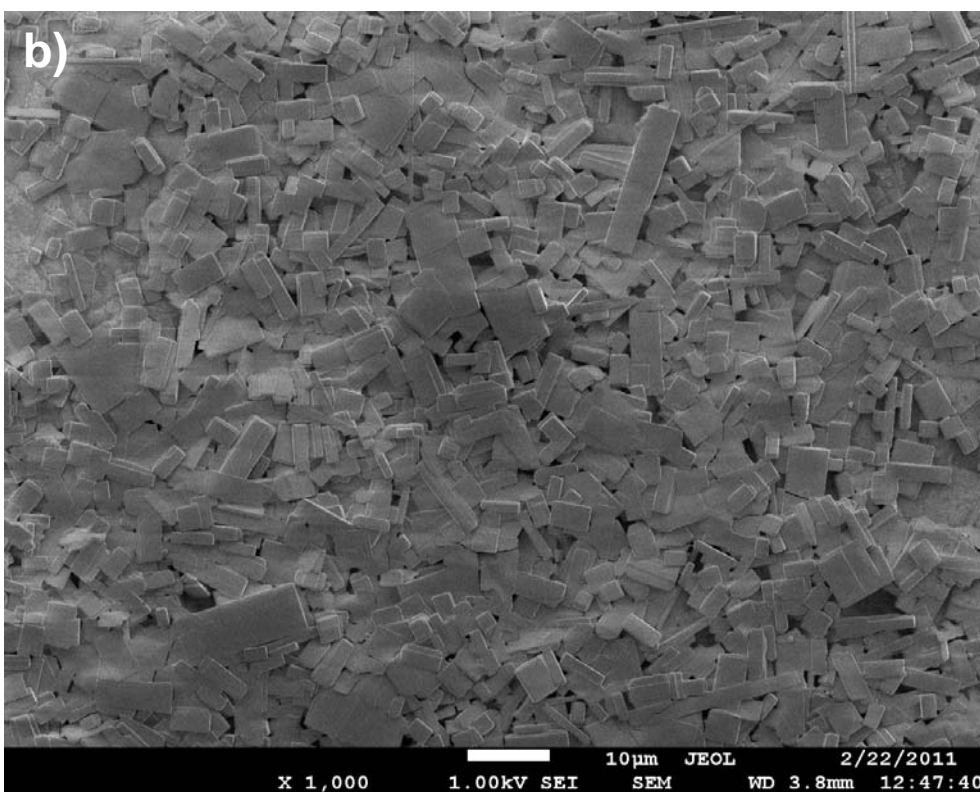
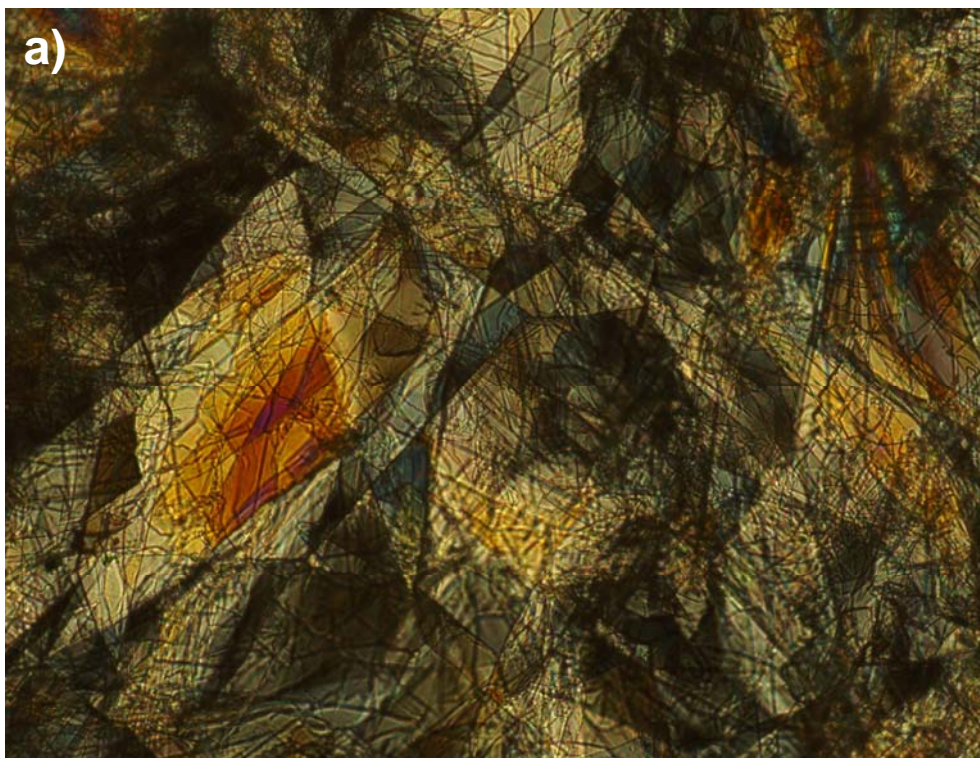


Figure ESI-5. Film of *nACh-I* prepared by casting from chloroform. a) Polarizing optical micrograph; b) SEM micrograph.

Methodology used for single-crystal analysis by X-ray diffraction.

A prismatic crystal (0.1 x 0.1 x 0.2 mm) was selected and mounted on a MAR345 diffractometer with an image plate detector. Unit-cell parameters were determined from 1141 reflections ($3 < \theta < 31^\circ$) and refined by least-squares method. Intensities were collected with graphite monochromatized Mo $K\alpha$ radiation, using φ -scan-technique. 6616 reflections were measured in the range $1.33 \leq \theta \leq 32.32$, 4395 of which were non-equivalent by symmetry ($R_{int}(on I) = 0.044$). 3094 reflections were assumed as observed applying the condition $I > 2\sigma(I)$. Lorentz-polarization and absorption corrections were made.

The structure was solved by direct methods, using SHELXS computer program and refined by full-matrix least-squares method with SHELX97 computer program, using 6616 reflections, (very negative intensities were not considered). The function minimized was $\sum w ||F_o|^2 - |F_c|^2|^2$, where $w = [\sigma^2(I) + (0.0262P)^2 + 1.8301P]^{-1}$, and $P = (|F_o|^2 + 2|F_c|^2)/3$, f , f' and f'' were taken from International Tables of X-Ray Crystallography.¹ All H atoms were computed and refined, using a riding model, with an isotropic temperature factor equal to 1.2 times the equivalent temperature factor of the atom to which are linked. The final $R(on F)$ factor was 0.052, $wR(on |F|^2) = 0.098$ and goodness of fit = 1.191 for all observed reflections. Number of refined parameters was 244. Max. shift/esd = 0.00, Mean shift/esd = 0.00. Max. and min. peaks in final difference synthesis was 0.358 and $-0.439 \text{ e}\text{\AA}^{-3}$, respectively.

Regarding the crystal refinement parameter for the structural resolution, only reflections that have a value max of $\theta = 25^\circ$ (ACTA 50) have been considered. Reflections between 25° and 32° have not been taken into account due to their poor quality. Lack of quality in reflections above 25° is due to the fact that the crystal does not diffract very well and to the limitations in the kind of detector (image plate with spindle axis only) that was used. Further attempts of crystallization were done, but no single crystals of better quality could be obtained.

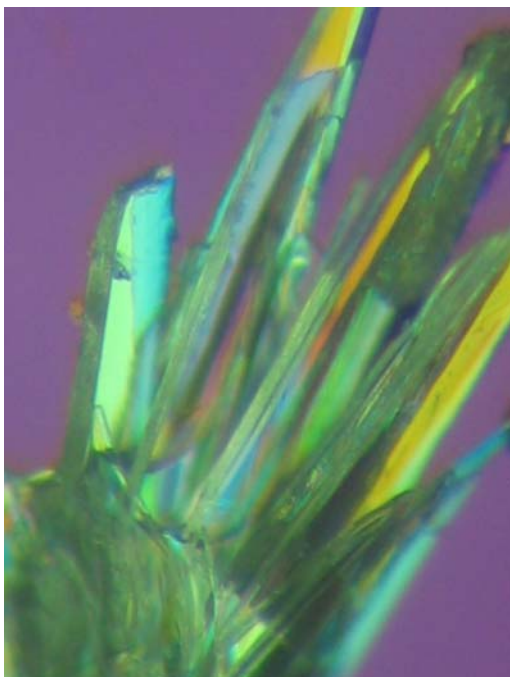


Figure ESI-6. Optical microscope image from single-crystal of 18ACh-I obtained from vapor-diffusion technique.

Table ESI-2. Crystal data and structure refinement of 18ACh·I.

Empirical formula	C ₂₃ H ₄₈ I N O ₂
Formula weight	497.52
Temperature	293(2) K
Wavelength	0.71073 Å
Crystal system, space group	Triclinic, P $\bar{1}$
Unit cell dimensions	a = 5.759(6) Å; α = 83.07(5) $^\circ$ b = 7.670(6) Å; β = 87.04(5) $^\circ$ c = 30.89(2) Å; γ = 89.32(5) $^\circ$.
Volume	1353(2) Å ³
Z, Calculated density	2, 1.221 Mg/m ³
Absorption coefficient	1.199 mm ⁻¹
F(000)	524
Crystal size	0.2 x 0.1 x 0.07 mm
Theta range for data collection	1.33 to 32.32 $^\circ$.
Limiting indices	-8 \leq h \leq 8, -11 \leq k \leq 11, -43 \leq l \leq 46
Reflections collected / unique	6616 / 4395 [R(int) = 0.0441]
Completeness to theta = 25.00	61.6 %
Absorption correction	Empirical
Max. and min. transmission	0.92 and 0.87
Refinement method	Full-matrix least-squares on F ²
Data / restraints / parameters	4395 / 0 / 244
Goodness-of-fit on F ²	1.191
Final R indices [$I > 2\sigma(I)$]	R1 = 0.0524, wR2 = 0.0984
R indices (all data)	R1 = 0.0821, wR2 = 0.1167
Largest diff. peak and hole	0.358 and -0.439 e.Å ⁻³

Reference: In *International Tables of X-Ray Crystallography, Vol. IV*; Ibers J.A.; Hamilton W.C., Ed., Kynoch press: Birmingham, 1974; pp. 99-100 and 149.

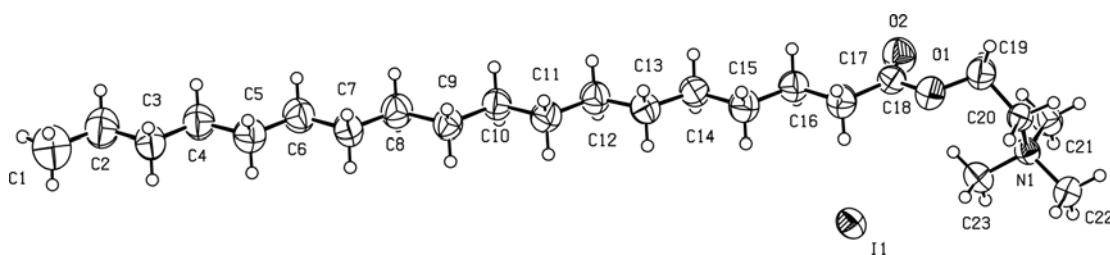


Figure ESI-7. ORTEP representation of the 18ACh·I molecule conformation in the crystal obtained from vapor-diffusion technique.

Table ESI-3. Atomic coordinates ($\times 10^4$) and equivalent isotropic displacement parameters ($\text{\AA}^2 \cdot 10^3$) for 18ACh-I; U(eq) is defined as one third of the trace of the orthogonalized U_{ij} tensor.

Atom	Atomic coordinates ($\times 10^4$)			U (eq)
	x	y	z	
I (1)	8586 (1)	7143 (1)	669 (1)	62 (1)
O (1)	13855 (8)	10032 (6)	1632 (1)	65 (1)
O (2)	10090 (9)	10809 (7)	1732 (2)	81 (2)
N (1)	14657 (8)	12166 (6)	666 (1)	45 (1)
C (1)	-7817 (18)	-13183 (13)	4722 (3)	135 (4)
C (2)	-7729 (15)	-11224 (12)	4550 (3)	112 (3)
C (3)	-5389 (13)	-10592 (9)	4368 (2)	79 (2)
C (4)	-5409 (13)	-8641 (9)	4202 (2)	80 (2)
C (5)	-3028 (13)	-7923 (10)	4016 (2)	79 (2)
C (6)	-3021 (13)	-5977 (9)	3845 (2)	79 (2)
C (7)	-640 (12)	-5305 (9)	3659 (2)	71 (2)
C (8)	-663 (13)	-3388 (9)	3483 (2)	75 (2)
C (9)	1676 (11)	-2632 (9)	3292 (2)	66 (2)
C (10)	1642 (11)	-683 (8)	3119 (2)	64 (2)
C (11)	4039 (11)	-6 (9)	2950 (2)	67 (2)
C (12)	4032 (11)	1930 (8)	2774 (2)	68 (2)
C (13)	6433 (11)	2665 (8)	2611 (2)	65 (2)
C (14)	6418 (11)	4579 (8)	2418 (2)	64 (2)
C (15)	8799 (12)	5243 (9)	2232 (2)	71 (2)
C (16)	8892 (11)	7178 (8)	2066 (2)	63 (2)
C (17)	11281 (12)	7775 (9)	1884 (2)	70 (2)
C (18)	11582 (13)	9691 (9)	1751 (2)	55 (2)
C (19)	14471 (2)	11845 (9)	1510 (2)	69 (2)
C (20)	15952 (9)	11999 (8)	1085 (2)	48 (1)
C (21)	13196 (11)	13779 (8)	618 (2)	65 (2)
C (22)	16458 (10)	12305 (8)	289 (2)	59 (2)
C (23)	13156 (11)	10618 (8)	640 (2)	63 (2)

Table ESI-4. Bond lengths [Å] and angles [°] for 18ACh·I.

O(1)-C(18)	1.362(7)
C(21)-H(21A)	0.9600
C(21)-H(21B)	0.9600
C(21)-H(21C)	0.9600
C(22)-H(22A)	0.9600
C(22)-H(22B)	0.9600
C(22)-H(22C)	0.9600
C(23)-H(23A)	0.9600
C(23)-H(23B)	0.9600
C(23)-H(23C)	0.9600
C(18)-O(1)-C(19)	116.8(5)
C(21)-N(1)-C(23)	108.7(5)
C(21)-N(1)-C(22)	107.8(4)
C(23)-N(1)-C(22)	108.9(4)
C(21)-N(1)-C(20)	111.7(4)
C(23)-N(1)-C(20)	112.1(4)
C(22)-N(1)-C(20)	107.5(4)
C(2)-C(1)-H(1A)	109.5
C(2)-C(1)-H(1B)	109.5
H(1A)-C(1)-H(1B)	109.5
C(2)-C(1)-H(1C)	109.5
H(1A)-C(1)-H(1C)	109.5
H(1B)-C(1)-H(1C)	109.5
C(3)-C(2)-C(1)	114.4(8)
C(3)-C(2)-H(2A)	108.7
C(1)-C(2)-H(2A)	108.7
C(3)-C(2)-H(2B)	108.7
C(1)-C(2)-H(2B)	108.7
H(2A)-C(2)-H(2B)	107.6
C(2)-C(3)-C(4)	112.1(7)
C(2)-C(3)-H(3A)	109.2
C(4)-C(3)-H(3A)	109.2
C(2)-C(3)-H(3B)	109.2
C(4)-C(3)-H(3B)	109.2
H(3A)-C(3)-H(3B)	107.9
C(3)-C(4)-C(5)	114.0(6)
C(3)-C(4)-H(4A)	108.8
C(5)-C(4)-H(4A)	108.8
C(3)-C(4)-H(4B)	108.8
C(5)-C(4)-H(4B)	108.8
H(4A)-C(4)-H(4B)	107.7
C(6)-C(5)-C(4)	114.6(6)
C(6)-C(5)-H(5A)	108.6
C(4)-C(5)-H(5A)	108.6
C(6)-C(5)-H(5B)	108.6
C(4)-C(5)-H(5B)	108.6
H(5A)-C(5)-H(5B)	107.6
C(5)-C(6)-C(7)	113.5(6)
C(5)-C(6)-H(6A)	108.9
C(7)-C(6)-H(6A)	108.9
C(5)-C(6)-H(6B)	108.9
C(7)-C(6)-H(6B)	108.9
H(6A)-C(6)-H(6B)	107.7
C(8)-C(7)-C(6)	113.1(6)
C(8)-C(7)-H(7A)	109.0
C(6)-C(7)-H(7A)	109.0
C(8)-C(7)-H(7B)	109.0

C(6)-C(7)-H(7B)	109.0
H(7A)-C(7)-H(7B)	107.8
C(7)-C(8)-C(9)	115.6(6)
C(7)-C(8)-H(8A)	108.4
C(9)-C(8)-H(8A)	108.4
C(7)-C(8)-H(8B)	108.4
C(9)-C(8)-H(8B)	108.4
H(8A)-C(8)-H(8B)	107.4
C(10)-C(9)-C(8)	115.3(6)
C(10)-C(9)-H(9A)	108.5
O(1)-C(19)	1.440(7)
O(2)-C(18)	1.205(7)
N(1)-C(21)	1.485(8)
N(1)-C(23)	1.490(7)
N(1)-C(22)	1.515(7)
N(1)-C(20)	1.517(6)
C(1)-C(2)	1.532(12)
C(1)-H(1A)	0.9600
C(1)-H(1B)	0.9600
C(1)-H(1C)	0.9600
C(2)-C(3)	1.496(10)
C(2)-H(2A)	0.9700
C(2)-H(2B)	0.9700
C(3)-C(4)	1.522(9)
C(3)-H(3A)	0.9700
C(3)-H(3B)	0.9700
C(4)-C(5)	1.541(9)
C(4)-H(4A)	0.9700
C(4)-H(4B)	0.9700
C(5)-C(6)	1.522(9)
C(5)-H(5A)	0.9700
C(5)-H(5B)	0.9700
C(6)-C(7)	1.531(9)
C(6)-H(6A)	0.9700
C(6)-H(6B)	0.9700
C(7)-C(8)	1.505(9)
C(7)-H(7A)	0.9700
C(7)-H(7B)	0.9700
C(8)-C(9)	1.534(8)
C(8)-H(8A)	0.9700
C(8)-H(8B)	0.9700
C(9)-C(10)	1.526(8)
C(9)-H(9A)	0.9700
C(9)-H(9B)	0.9700
C(10)-C(11)	1.525(8)
C(10)-H(10A)	0.9700
C(10)-H(10B)	0.9700
C(11)-C(12)	1.518(9)
C(11)-H(11A)	0.9700
C(11)-H(11B)	0.9700
C(12)-C(13)	1.537(8)
C(12)-H(12A)	0.9700
C(12)-H(12B)	0.9700
C(13)-C(14)	1.516(8)
C(13)-H(13A)	0.9700
C(13)-H(13B)	0.9700
C(14)-C(15)	1.529(8)
C(14)-H(14A)	0.9700
C(14)-H(14B)	0.9700
C(15)-C(16)	1.511(9)

C(15)-H(15A)	0.9700
C(15)-H(15B)	0.9700
C(16)-C(17)	1.514(8)
C(16)-H(16A)	0.9700
C(16)-H(16B)	0.9700
C(17)-C(18)	1.487(9)
C(17)-H(17A)	0.9700
C(17)-H(17B)	0.9700
C(19)-C(20)	1.523(8)
C(19)-H(19A)	0.9700
C(19)-H(19B)	0.9700
C(20)-H(20A)	0.9700
C(20)-H(20B)	0.9700
C(8)-C(9)-H(9A)	108.5
C(10)-C(9)-H(9B)	108.5
C(8)-C(9)-H(9B)	108.5
H(9A)-C(9)-H(9B)	107.5
C(11)-C(10)-C(9)	112.4(6)
C(11)-C(10)-H(10A)	109.1
C(9)-C(10)-H(10A)	109.1
C(11)-C(10)-H(10B)	109.1
C(9)-C(10)-H(10B)	109.1
H(10A)-C(10)-H(10B)	107.8
C(12)-C(11)-C(10)	113.1(6)
C(12)-C(11)-H(11A)	109.0
C(10)-C(11)-H(11A)	109.0
C(12)-C(11)-H(11B)	109.0
C(10)-C(11)-H(11B)	109.0
H(11A)-C(11)-H(11B)	107.8
C(11)-C(12)-C(13)	114.4(6)
C(11)-C(12)-H(12A)	108.7
C(13)-C(12)-H(12A)	108.7
C(11)-C(12)-H(12B)	108.7
C(13)-C(12)-H(12B)	108.7
H(12A)-C(12)-H(12B)	107.6
C(14)-C(13)-C(12)	114.5(6)
C(14)-C(13)-H(13A)	108.6
C(12)-C(13)-H(13A)	108.6
C(14)-C(13)-H(13B)	108.6
C(12)-C(13)-H(13B)	108.6
H(13A)-C(13)-H(13B)	107.6
C(13)-C(14)-C(15)	113.4(6)
C(13)-C(14)-H(14A)	108.9
C(15)-C(14)-H(14A)	108.9
C(13)-C(14)-H(14B)	108.9
C(15)-C(14)-H(14B)	108.9
H(14A)-C(14)-H(14B)	107.7
C(16)-C(15)-C(14)	115.0(6)
C(16)-C(15)-H(15A)	108.5
C(14)-C(15)-H(15A)	108.5
C(16)-C(15)-H(15B)	108.5
C(14)-C(15)-H(15B)	108.5
H(15A)-C(15)-H(15B)	107.5
C(15)-C(16)-C(17)	113.1(6)
C(15)-C(16)-H(16A)	109.0
C(17)-C(16)-H(16A)	109.0
C(15)-C(16)-H(16B)	109.0
C(17)-C(16)-H(16B)	109.0
H(16A)-C(16)-H(16B)	107.8
C(18)-C(17)-C(16)	116.6(6)

C(18)-C(17)-H(17A)	108.1
C(16)-C(17)-H(17A)	108.1
C(18)-C(17)-H(17B)	108.1
C(16)-C(17)-H(17B)	108.1
H(17A)-C(17)-H(17B)	107.3
O(2)-C(18)-O(1)	123.1(6)
O(2)-C(18)-C(17)	127.4(6)
O(1)-C(18)-C(17)	109.5(6)
O(1)-C(19)-C(20)	108.8(5)
O(1)-C(19)-H(19A)	109.9
C(20)-C(19)-H(19A)	109.9
O(1)-C(19)-H(19B)	109.9
C(20)-C(19)-H(19B)	109.9
H(19A)-C(19)-H(19B)	108.3
N(1)-C(20)-C(19)	116.6(5)
N(1)-C(20)-H(20A)	108.1
C(19)-C(20)-H(20A)	108.1
N(1)-C(20)-H(20B)	108.1
C(19)-C(20)-H(20B)	108.1
H(20A)-C(20)-H(20B)	107.3
N(1)-C(21)-H(21A)	109.5
N(1)-C(21)-H(21B)	109.5
H(21A)-C(21)-H(21B)	109.5
N(1)-C(21)-H(21C)	109.5
H(21A)-C(21)-H(21C)	109.5
H(21B)-C(21)-H(21C)	109.5
N(1)-C(22)-H(22A)	109.5
N(1)-C(22)-H(22B)	109.5
H(22A)-C(22)-H(22B)	109.5
N(1)-C(22)-H(22C)	109.5
H(22A)-C(22)-H(22C)	109.5
H(22B)-C(22)-H(22C)	109.5
N(1)-C(23)-H(23A)	109.5
N(1)-C(23)-H(23B)	109.5
H(23A)-C(23)-H(23B)	109.5
N(1)-C(23)-H(23C)	109.5
H(23A)-C(23)-H(23C)	109.5
H(23B)-C(23)-H(23C)	109.5

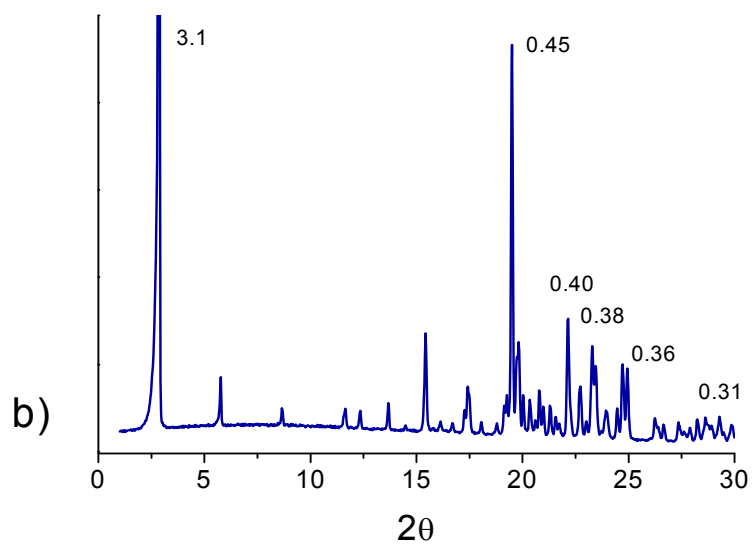
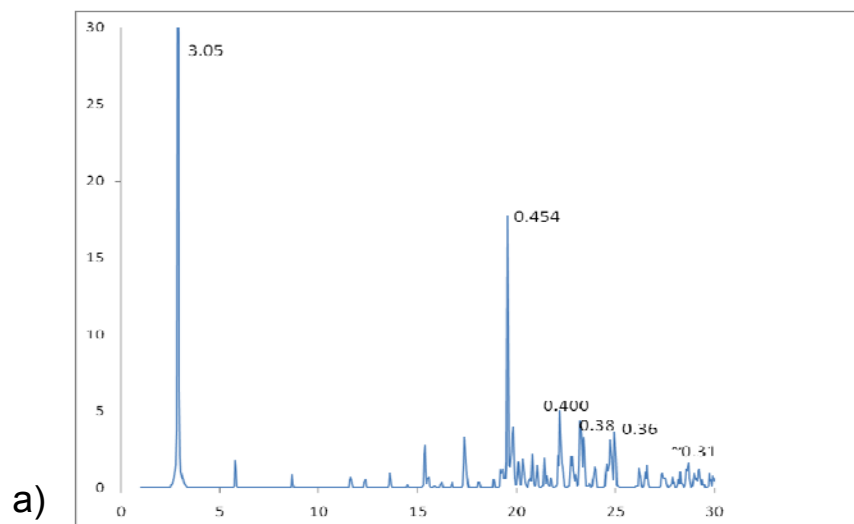


Figure ESI-8. Compared X-ray diffraction profiles of Ph-I α of 18ACh-I. a) Simulated for the crystal lattice determined from the monocrystal by direct method. b) Obtained from annealed powder sample.

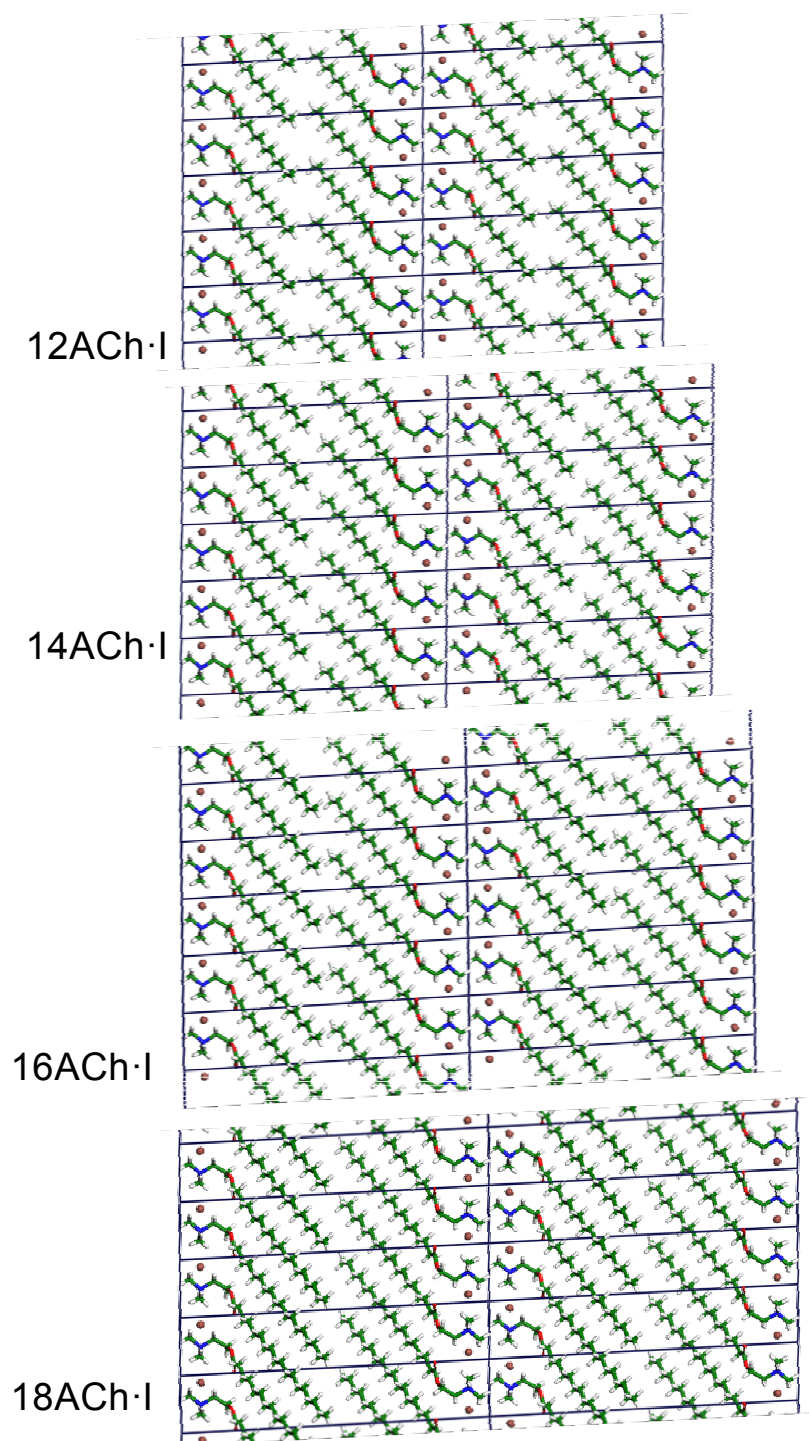
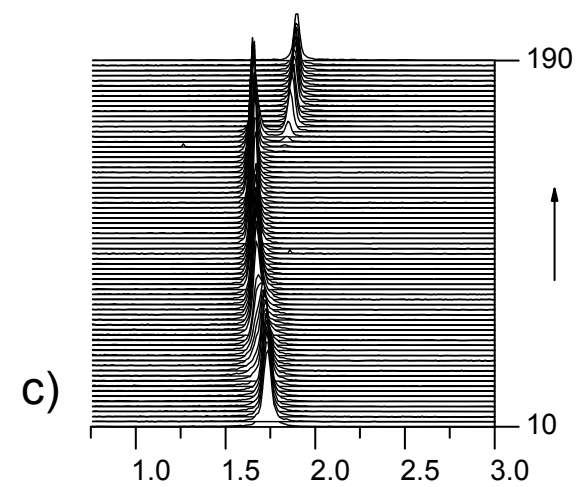
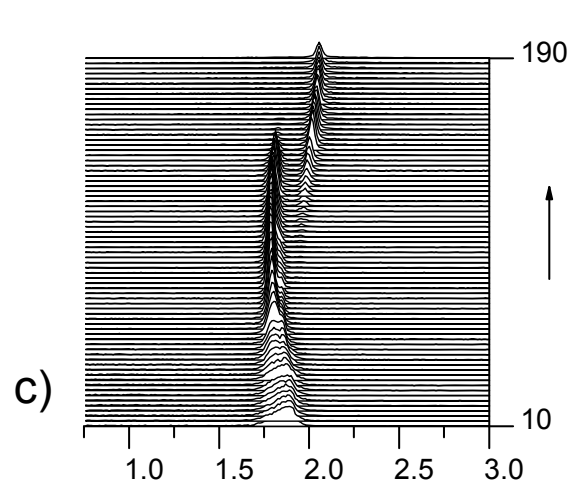
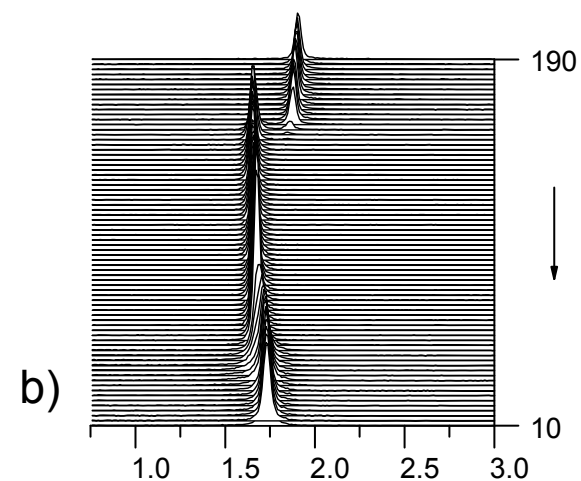
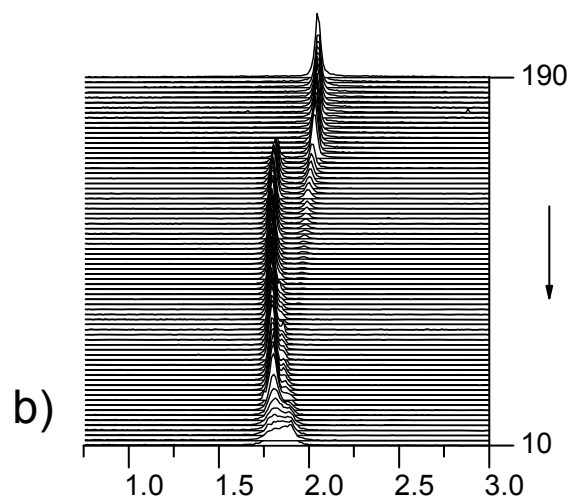
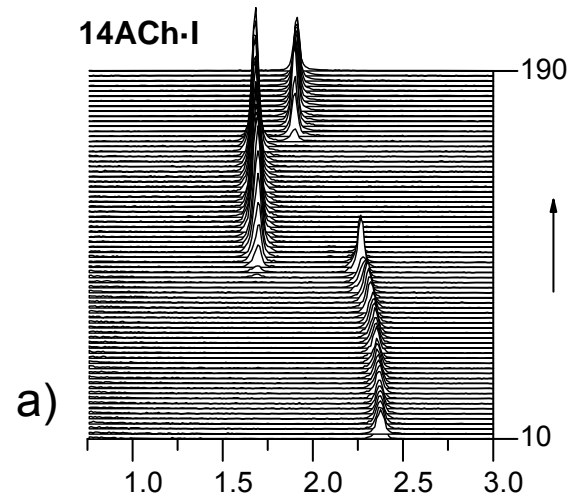
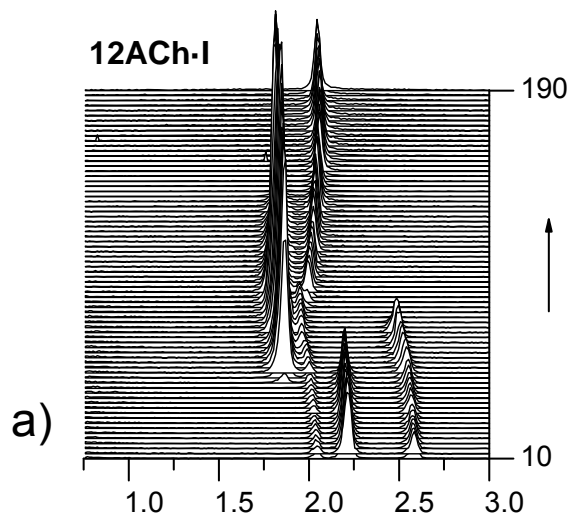
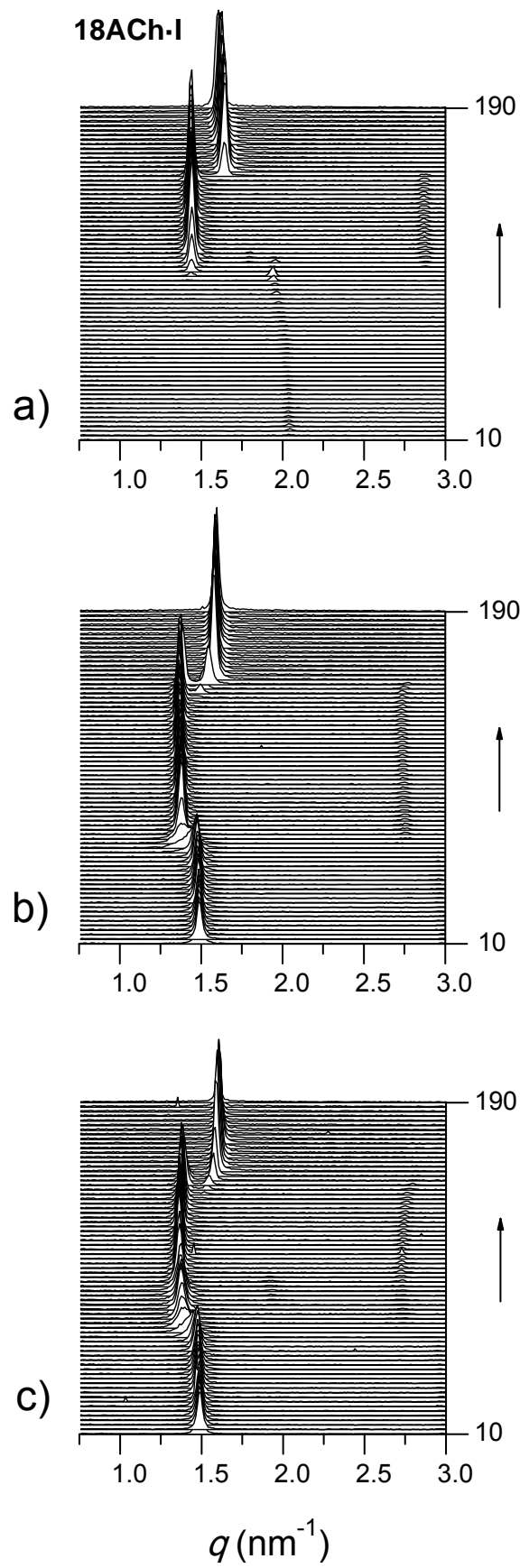


Figure ESI-9. Crystal models of phase Ph-I α of *n*ACh·I viewed along down *b*-axis. Ten unit cells are visualized for each compound.



q (nm⁻¹)

q (nm⁻¹)



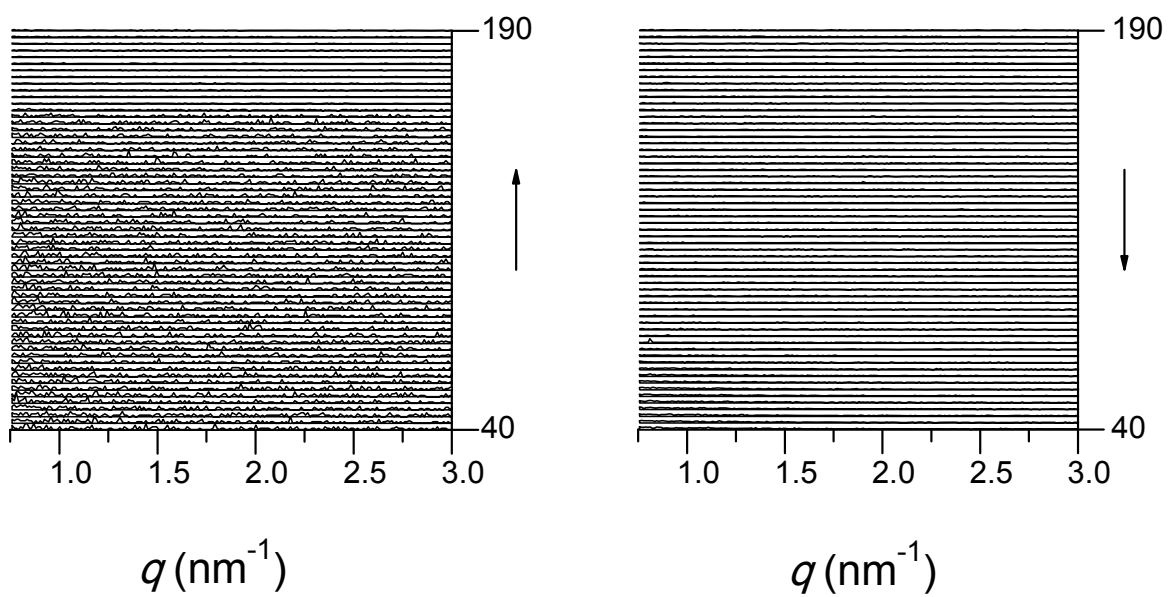
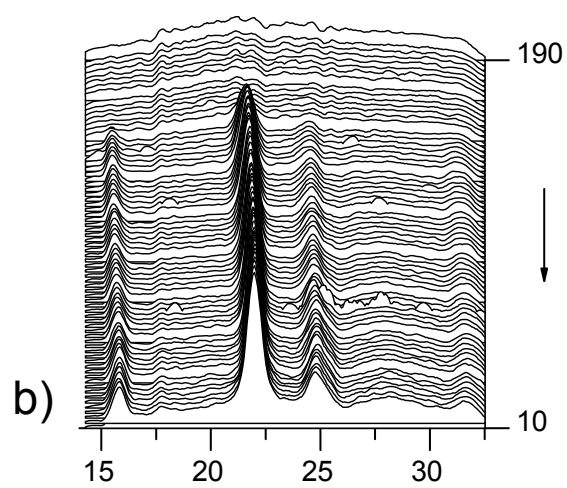
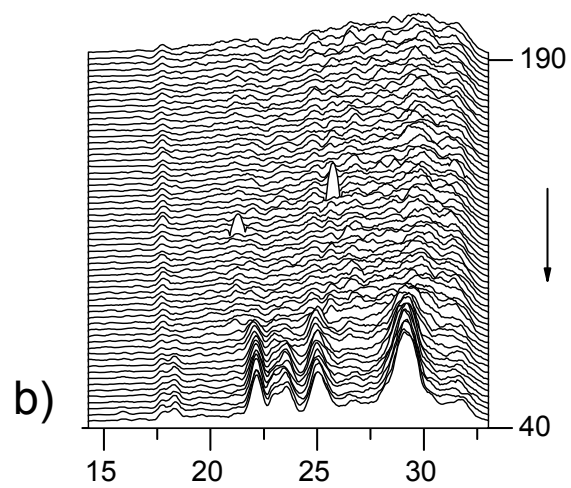
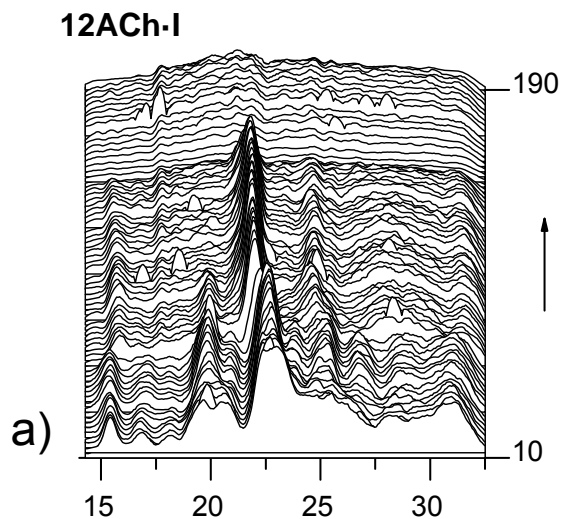
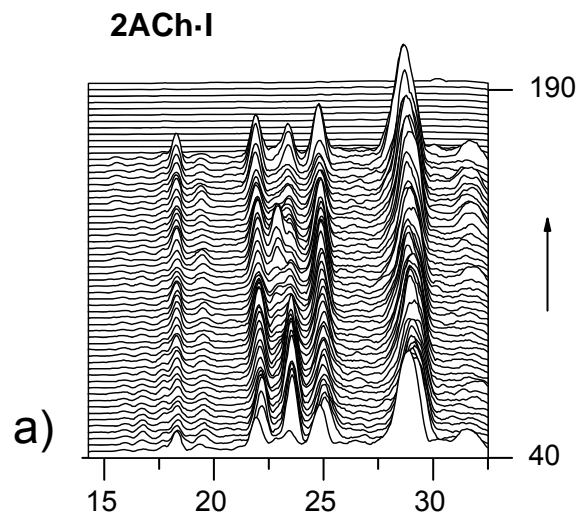
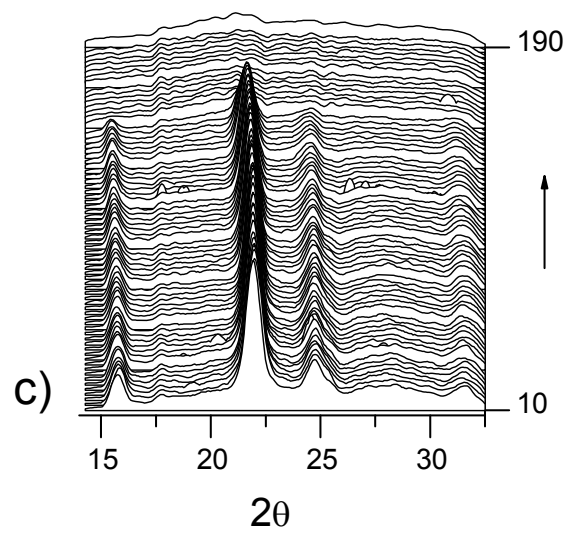


Figure ESI-10. SAXS plots from 12, 14 and 18ACh·I and ·2ACh·I registered at heating from room temperature (a), cooling (b) and reheating (c). No signs were observed in SAXS region for 2ACh·I.



2θ



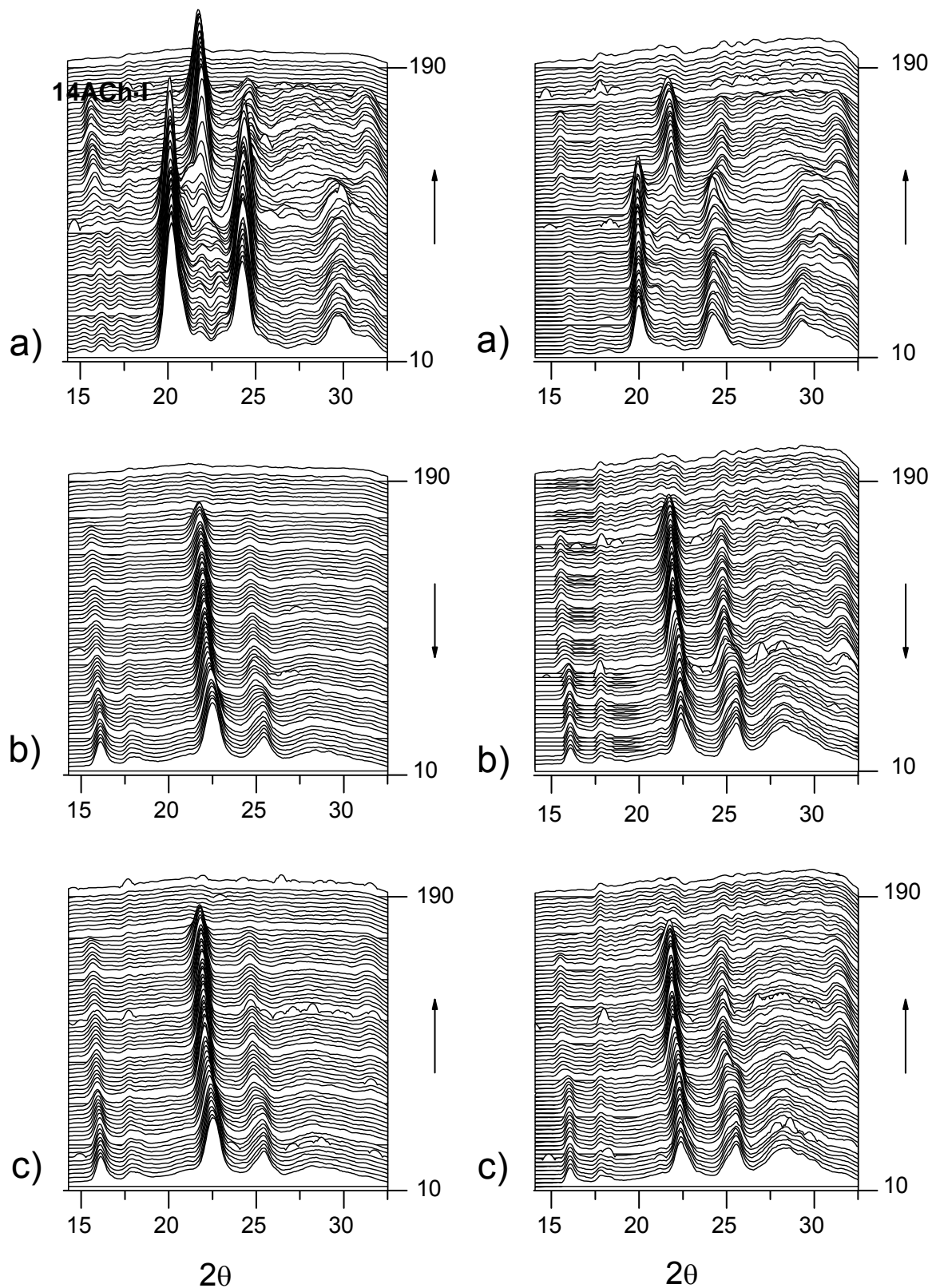


Figure ESI-11. WAXS plots from 2, 12, 14 and 18ACh-I registered at heating from room temperature (a), cooling (b) and reheating (c).

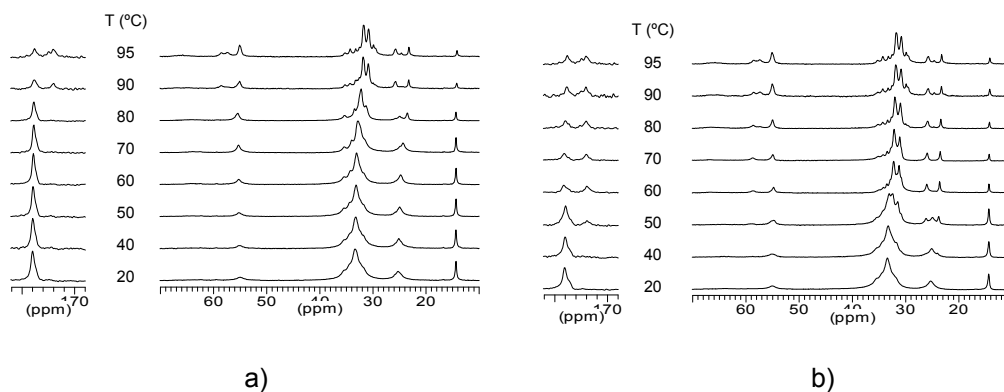


Figure ESI-12. ^{13}C CP/MAS NMR spectra of 14ACh·I registered at the indicated temperatures. a) At heating and b) at cooling.

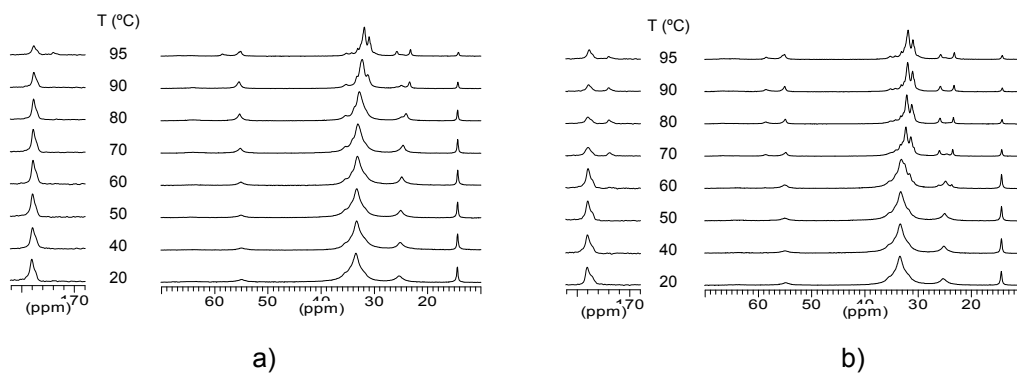


Figure ESI-13. ^{13}C CP/MAS NMR spectra of 16ACh·I registered at the indicated temperatures. a) At heating and b) at cooling.

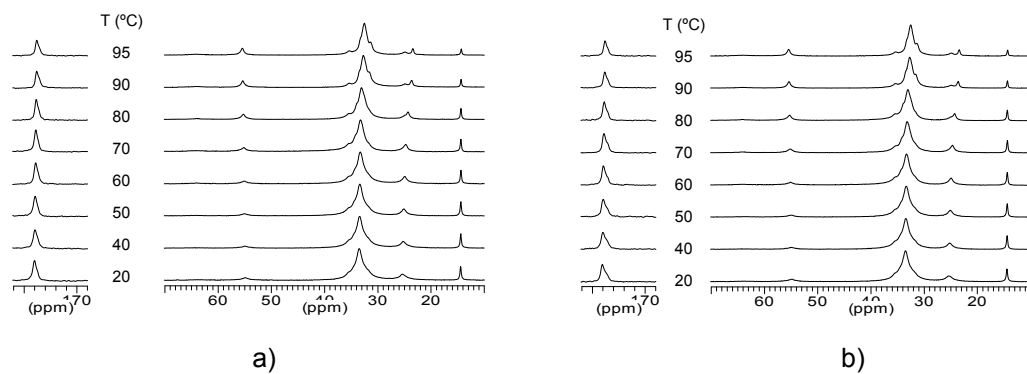


Figure ESI-14. ^{13}C CP/MAS NMR spectra of 18ACh·I registered at the indicated temperatures. a) At heating and b) at cooling.

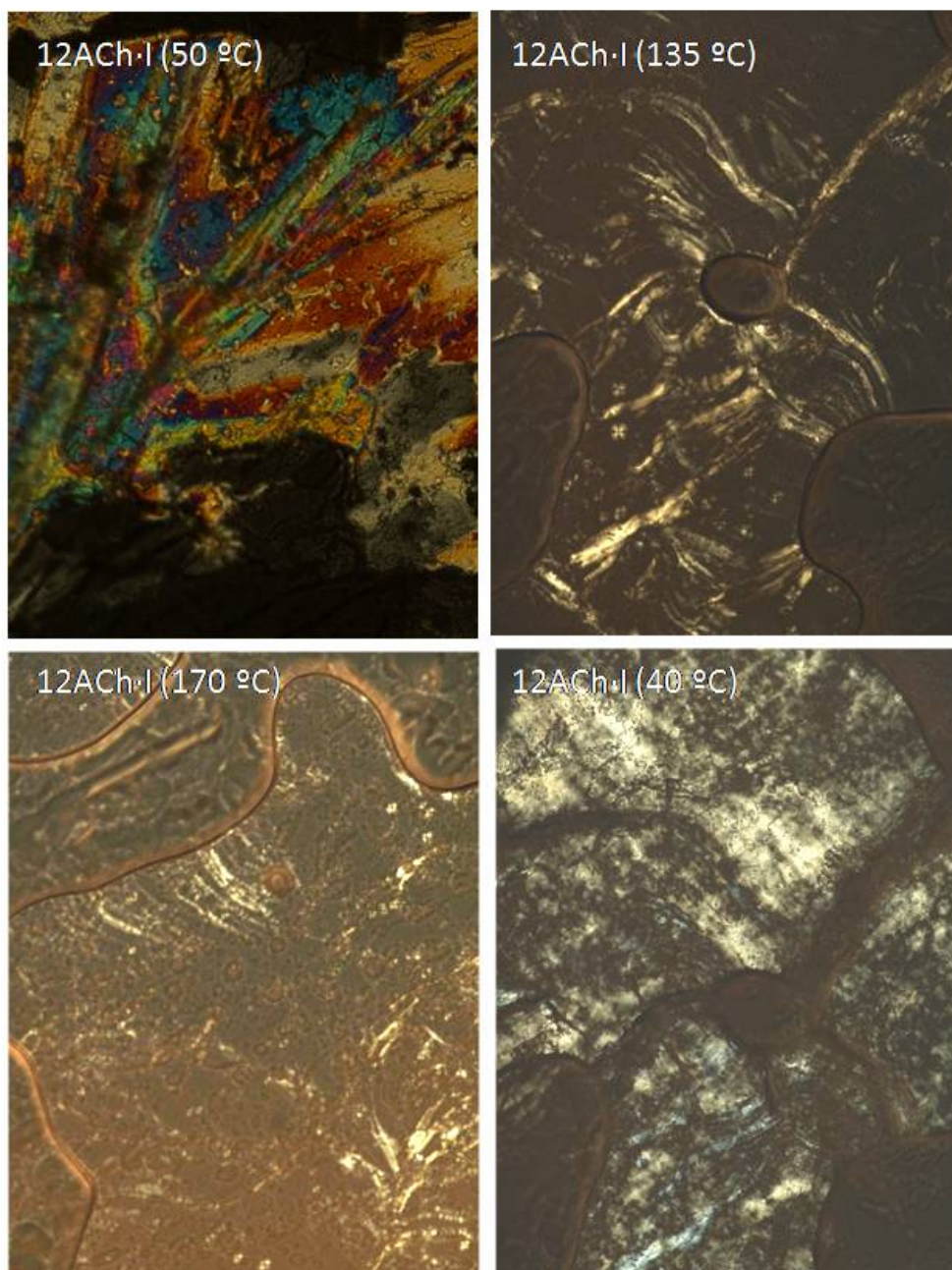


Figure ESI-15. POM pictures of 12ACh-I at the indicated temperatures (the last one taken after cooling from high temperature).

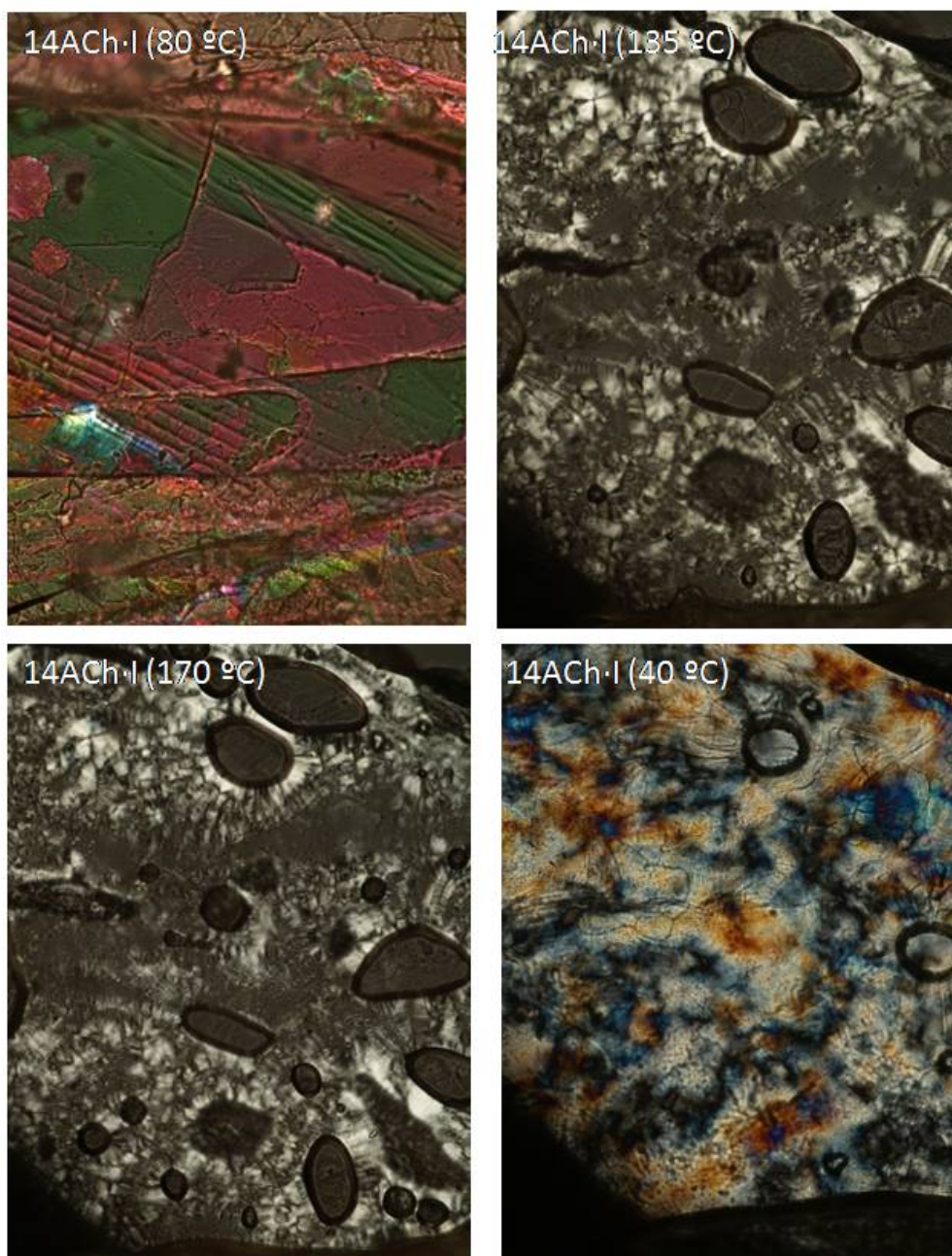


Figure ESI-16. POM pictures of 14ACh-I at the indicated temperatures (the last one taken after cooling from high temperature).

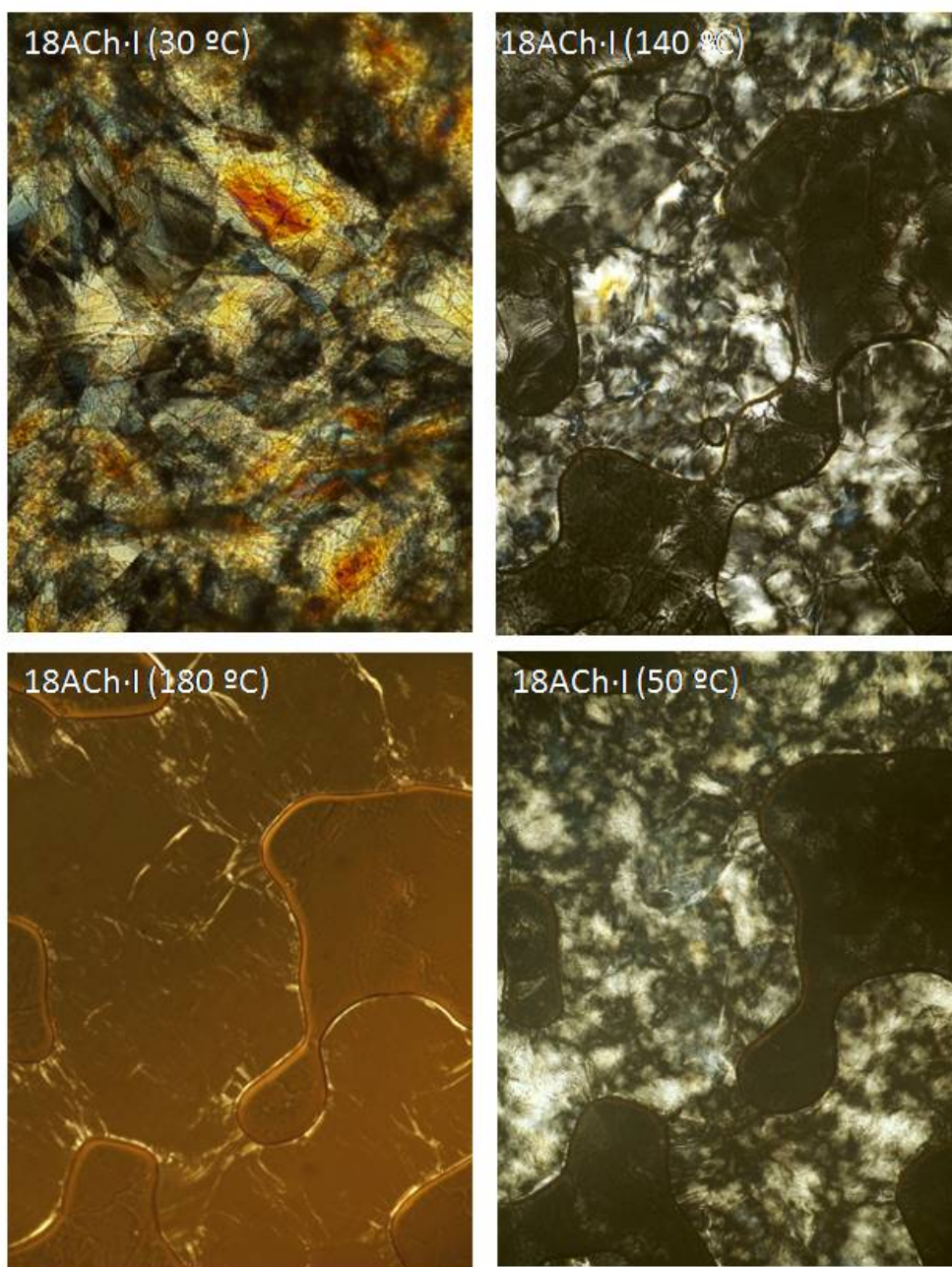


Figure ESI-17. POM pictures of 18ACh-I at the indicated temperatures (the last one taken after cooling from high temperature).
